PERGAMON

International Journal of Heat and Mass Transfer 44 (2001) 2277–2285

International Journal of HEAT and MASS TRANSFER

www.elsevier.com/locate/ijhmt

Turbulent heat transfer with phase change material suspensions

Sanjay K. Roy *, Branko L. Avanic

PhD Research Group, Inc., P.O. Box 248433, Coral Gables, FL 33124, USA

Received 10 December 1999; received in revised form 25 July 2000

Abstract

This paper presents an effective specific heat capacity model for turbulent heat transfer to phase change material (PCM) suspensions in a circular tube with constant wall heat flux. The model has been implemented in the form of a computer code and its numerical predictions are found to agree with previously published experimental data. Further results show that the bulk Stefan number, the non-dimensional melt temperature range and the degree of subcooling are the three parameters of importance. They also confirm that considerable reductions in wall temperatures, of the order of 50% or more, may be obtained at low to moderate Stefan numbers. For most typical cases with high wall heat fluxes, the Stefan number and the degree of subcooling determine the location of the tube where the phase change effects are predominant.

1. Introduction

Phase change material (PCM) suspensions have been the subject of a number of studies over the past decade due to possible applications in heat transfer and energy storage systems (e.g. [1]). Although most investigations have been targeted towards practical applications, limited theoretical modeling has also been done to support the experimental work. Early models considered the case of zero subcooling of the PCM and were based on ideal PCMs melting at a constant temperature. Later experiments showed that these assumptions were unrealistic, and effects of subcooling and finite melt temperature ranges have been considered in more recent models (e.g. [2]).

All previous theoretical models have considered laminar heat transfer situations. In contrast, a vast majority of engineering applications of PCM suspensions are expected to involve turbulent flows. Thus, the case of turbulent heat transfer to a fully developed flow in a circular duct with constant wall heat flux is considered in this paper. This standard configuration has been selected at this stage since experimental results are available and can be used to validate the model. It is expected that the verified numerical model will be used to study more complex problems as required in the future.

2. Governing equations

An effective specific heat approach, recently verified for laminar heat transfer [3], is being used since it can be more easily implemented in practice. In the proposed method, the phase change effects are directly incorporated into the energy equation by assuming the specific heat capacity to be a function of the temperature. Thus, as a first step, the governing equation and boundary conditions for the problem can be written in the Reynolds-averaged form as

$$u\frac{\partial T}{\partial Z}=\frac{1}{r\rho c_{\mathrm{p}}}\frac{\partial}{\partial r}\left[rk\left(\frac{\partial T}{\partial r}\right)\right]+\frac{1}{r}\frac{\partial}{\partial r}\left[r\varepsilon_{\mathrm{H}}\left(\frac{\partial T}{\partial r}\right)\right]$$

with $T=T_{\mathrm{i}}$ at $z=0$,

$\partial T/\partial r=0$ at $r=0$, and $-k\partial T/\partial r=0-q_{\mathrm{w}}$ at $r=R$.

* Corresponding author. Tel.: +1-305-665-7415; fax: +1-305-665-8749.

E-mail address: sroy@phdresearch.com (S.K. Roy).

0017-9310/01/$ - see front matter
PII: S0017-9310(00)00260-X

Nomenclature

c	volumetric concentration of phase change material in suspension
c_m	mass concentration of phase change material in suspension
c_p	specific heat capacity (of suspension, unless otherwise specified)
$c_{p,ND}$	heat capacity ratio ($= c_m c_{p,PCM}/c_p$)
h_{fs}	latent heat of melting
k	thermal conductivity of suspension
q	heat flux
r	radial coordinate
u	velocity
z	axial coordinate
A^+	empirical constant in van Driest relation
D	diameter of tube
K	empirical constant in van Driest relation
Mr	non-dimensional melt temperature range ($= (T_{MPH} - T_i)/(q_w R/k)$)
Pr	Prandtl number ($= \nu/\alpha$)
R	radius of tube
Re	Reynolds number ($= u_m D/\nu$)
Sb	degree of subcooling ($= (T_{MPL} - T_i)/(q_w R/k)$)
Ste	bulk Stefan number ($= c_p(q_w R/k)/(c_m h_{fs})$)
T	temperature
α	thermal diffusivity of the suspension
ε_H	eddy diffusivity
ε_M	momentum eddy diffusivity
ν	kinematic viscosity of suspension
ρ	density of suspension
τ	shear stress

Superscripts/subscripts

$*$ $+$	non-dimensional variable
COR	corrected for temperature effects on viscosity
CP	constant property
ND	non-dimensional property ratio
MPH	"higher" melting point
MPL	"lower" melting point
PCM	phase change material
i	inlet
l	suspending liquid
m	mean
w	wall
z	location z along the axial direction on tube

In the above equation, u is the Reynolds-averaged velocity in the flow direction, T the Reynolds-averaged temperature, z the flow direction, r the radial coordinate, R the radius of the tube, q_w the wall heat flux, k the thermal conductivity, ρ the density, c_p the specific heat capacity and ε_H is the eddy diffusivity associated with the turbulent heat transfer process. The property values in the above equation are those of the suspension and can be derived relatively easily since a typical PCM suspension with very small particles/microcapsules behaves like a homogeneous fluid (e.g. an 10% *n*-octadecane in water emulsion appears very similar to milk). Under these circumstances, they can be evaluated from the fluid and phase change material properties and the concentration of the phase change material in the suspension.

Suspension density. The density of any suspension is equal to the volume-averaged density of the constituents (e.g. [4]). In order to ensure long-term stability of a suspension however, the density of the phase change material and the suspending fluid are expected to be similar for most practical applications. As a result, the ratio of the phase change material density to the suspension density can be approximated as unity in developing the theoretical model. Furthermore, since the densities of most phase change materials in their liquid and solid phases differ by 10–15% or less, the suspension density will not change by more than 1–2% for phase change material concentrations of 10–20%, and can be assumed to be a constant. Thus, changes in volumetric concentration of the phase change material due to these density variations will also be negligible.

Suspension thermal conductivity. The thermal conductivity of stationary suspensions can be evaluated as a function of volumetric concentration by using standard correlations [4]. Unlike laminar flows however, no additional enhancement factors are required [5] since turbulent mixing effects are directly incorporated in the eddy diffusivity term. The thermal conductivity of the suspension can be assumed to be a constant since the thermal conductivity of the phase change material typically does not change significantly during the phase change process. Even if this variation were to be of the order of 20–30%, the overall effect would be quite small due to the low (10–20%) volumetric concentrations of the phase change material in a typical PCM suspension. As an example consider the case of a 10% *n*-hexadecane in water suspension: if the thermal conductivity of the PCM varies by 30% during the melting/solidification process, the change in overall suspension conductivity will be only 1.2%.

Suspension specific heat capacity. The specific heat capacity of the suspension must be evaluated more carefully in order to account for the phase change effects. In an effective specific heat model, the phase change material is assumed to melt over a finite temperature range so that the specific heat of the phase change material and the suspension will be functions of temperature. However, if the temperature dependence is

included in the specific heat capacity of the phase change material, $c_{p,PCM}$, elementary thermodynamic considerations show that the following equation can be used to calculate the suspension specific heat capacity for all temperatures

$$c_p = (1 - c_m)c_{p,l} + c_m c_{p,PCM}, \quad c_m = \left(\frac{\rho_{PCM}}{\rho}\right)c \approx c.$$

In this equation, c_m is the mass concentration and c the volumetric concentration of the phase change material and the subscripts l and PCM refer to the suspending fluid and phase change material, respectively.

In order to use the above equation, it is necessary to first define T_{MPL} and T_{MPH} as the temperatures at which melting is initiated (''lower'' melting point) and completed (''higher'' melting point). Outside this melt temperature range, (i.e. for $T < T_{MPL}$ and $T > T_{MPH}$), the specific heat of the suspension is the mass-averaged specific heat of its constituents [4]. Since the specific heat capacity of the phase change material in its solid and liquid phases are usually similar and do not vary significantly with temperature, it can be assumed to be a constant. Even if the difference between the liquid and solid phase heat capacities is large (e.g. about 25% for *n*-hexadecane), the low concentrations of the phase change material result in a overall variation of 2–5% or less (usually far lower when water, with its high specific heat capacity, is the suspending fluid). As a result, the specific heat capacity of the suspension, calculated using the above equation, can also be assumed to be a constant outside the melt temperature range.

In the melt temperature range itself, the specific heat capacity of the phase change material can be obtained from suitable analytical tests (e.g. differential scanning calorimetry (DSC)). This specific heat is related to the latent heat of melting, h_{fs}, through the following equation:

$$h_{fs} = \int_{T_{MPL}}^{T_{MPH}} C_{p,PCM}\, dT.$$

Previous studies with phase change material suspensions [3] show that the shape of the specific heat capacity–temperature curve has a very small effect on the heat transfer process (contrary to intuition, this is also true for latent heat energy storage systems [6] where one would expect such effects to be particularly noticeable). As a result, it is possible to assume that the specific heat capacity of the phase change material remains constant during the phase change process. Its effective value in the melt temperature range ($T_{MPL} \leqslant T \leqslant T_{MPH}$) is therefore given by the following equation:

$$C_{p,PCM} = \frac{h_{fs}}{T_{MPH} - T_{MPL}}.$$

This relation can now be used to calculate the specific heat capacity of the suspension in the melt temperature range using the equation given previously.

An important issue associated with the ''melt temperature range'' is the fact that it can be a function of both the particle size (i.e., where the melting is kinetics limited) as well as composition (and cooling history if the material tends to supercool). However, since the particle sizes in a typical PCM suspension are very small (<100 μm, $<10^{-9}$ kg), simple calculations show that the material will be effectively isothermal and melt kinetics will not have any impact in most cases. Composition related effects will be present for phase change materials which are mixtures, but the melt temperature range can be estimated using phase diagrams (based on a series of DSC tests for example [7]).

This issue becomes more complicated for many commercial/industrial grade materials which may contain small amounts of impurities. For such PCMs, it may not be worthwhile to develop a complete phase diagram and the best approach may be to conduct a DSC test to identify the various phase transitions. This can be followed by scoping type studies with various melt temperature ranges, say up to 1–2°C, at the different transitions. Results of these studies can then be used to obtain uncertainty estimates in the predictions. Combined experimental/numerical studies are probably required in this area to evaluate the limitations of this approach. Note that this problem will exist in any case regardless of the underlying mathematical formulation.

Finally, a few comments about DSC tests may be useful at this stage. As mentioned above, the specific heat during melting can be obtained by using suitable analytical tests. DSC is one such procedure which can be used to locate different phase transitions over a given temperature range. If properly calibrated and used, accurate determination of melting points (within ±0.5°C) and latent heats are possible using this technique (e.g. [7]). Note that the actual shape of the specific heat curve is not particularly important in this application.

Non-dimensionalization. All properties are now completely defined and it is advantageous to non-dimensionalize the problem in order to reduce the number of variables and minimize numerical errors at a later stage. Thus, the following non-dimensional variables are used:

$$T^* = (T - T_i)/(q_w R/k), \quad z^* = z/R, \quad r^* = r/R,$$
$$u^* = u/(\tau_w/\rho)^{1/2}.$$

The governing equations and boundary conditions therefore reduce to (after dropping the superscript *)

$$u\frac{\partial T}{\partial z} = \frac{1}{R^*}\left[\frac{\alpha_{ND}}{Pr}\frac{1}{r}\frac{\partial}{\partial r}\left[r\frac{\partial T}{\partial r}\right] + \frac{1}{r}\frac{\partial}{\partial r}\left[r\left(\frac{\varepsilon_H}{\nu}\right)\frac{\partial T}{\partial r}\right]\right]$$

with $T = 0$ at $z = 0$, $\partial T/\partial r = 0$ at $r = 0$, and $\partial T/\partial r = -1$ at $r = 1$.

In the above equation, Pr is the suspension Prandtl number ($Pr = \nu/\alpha$, ν being the kinematic viscosity and α is the thermal diffusivity of the suspension in the absence

of the phase change process). The parameter α_{ND} can be evaluated as a function of the non-dimensional temperature T:

$$\alpha_{ND} = 1 \quad \text{for } T < Sb$$

$$\alpha_{ND} = \frac{Ste\,Mr}{1 + Ste\,Mr(1 - c_{p,ND})}$$

for $Sb < T < Sb + Mr$, and

$$\alpha_{ND} = 1 \quad \text{for } T > Sb + Mr.$$

where Ste is the Stefan number $(= c_p(q_w R/k)/(c_m h_{fs}))$, Sb is the degree of subcooling $(= (T_{MPL} - T_i)/(q_w R/k))$, Mr is the non-dimensional melt range $(= (T_{MPH} - T_{MPL})/(q_w R/k))$, and $c_{p,ND}$ is the heat capacity ratio $(= c_m c_{p,PCM}/c_p)$.

The term R^+ in the non-dimensional energy conservation equation can be calculated from the following relation:

$$R^+ = \frac{R}{(v/\sqrt{\tau_w/\rho})} = \frac{Re\sqrt{f}}{4\sqrt{2}},$$

where Re is the Reynolds number $(= u_m D/v$, u_m the mean velocity and D the diameter) and f is the friction factor corresponding to this flow/Reynolds number.

Velocity distribution and other flow parameters. All flow related variables/parameters used in this study have been obtained from literature by assuming that the flow is Newtonian. Numerous previous studies with suspensions/emulsions (see for example, the discussion and references in [4]) confirm that this assumption is valid as long as the suspended particle sizes are very small and their volumetric concentrations are relatively low (less than 20–25%) as is the case with typical PCM suspensions. Thus, the friction factor f has been calculated using a very accurate explicit version of the classical Prandtl–Karman–Nikuradse correlation by Techo et al. [8]) (within ±0.1%):

$$\frac{1}{\sqrt{f}} = 0.8686 \ln\left(\frac{Re}{1.964 \ln Re - 3.8215}\right).$$

Three equations have been used to evaluate the velocity distribution in the duct. In the viscous sublayer $(r \geqslant 1 - 10.8/R^+)$, the non-dimensional velocity u is given by:

$$u = R^+[1 - r], \quad r \geqslant 1 - \frac{5}{R^+}$$

and [9]:

$$u = 5 \ln(R^+(1 - r)) + 3.05,$$
$$1 - 5/R^+ \leqslant r \leqslant 1 - 10.8/R^+.$$

Outside the viscous sublayer, turbulence effects dominate and the velocity distribution is given by

$$u^+ = 2.5 \ln\left[\frac{1.5R^+(1 - r^2)}{1 + 2r^2}\right] + 5.5.$$

The function ε_H/v is calculated by assuming that ε_H is equal to the momentum eddy diffusivity, ε_M (i.e. the turbulent Prandtl number is 1). Since the effective specific heat and thus the effective Prandtl number of the suspension is significantly greater than 1 during the phase change process, the van Driest approach [10] was used to evaluate the eddy diffusivity in the viscous sublayer

$$\frac{\varepsilon_M}{v} = \left[KR^+(1 - r)\left(1 - \exp\left(-\frac{R^+}{A^+}(1 - r^2)\right)\right)\right]^2 \left|\frac{\partial u}{\partial r}\right|,$$

where K and A^+ are empirical constants (= 0.4 and 26, respectively). Outside the viscous sublayer, the momentum eddy diffusivity have been calculated using:

$$\frac{\varepsilon_M}{v} = \frac{KR^+}{6}(1 - r^2)(1 + 2r^2), \quad K = 0.4.$$

3. Method of solution

A numerical approach was used to solve the governing equation with its boundary conditions. The energy equation was discretized using second-order central differences in the r-direction and first-order forward differences in the z-direction. Forward differences were also used to discretize the boundary conditions, and the overall set of algebraic equations were numerically solved using an implicit method. As a first step, the computer code implementing the model was verified for the case of a pure fluid using the correlation of Petukhov [11] which is considered to be the most accurate correlation for the configuration under consideration [8]. The maximum difference between the numerical results and the predicted values were less than 10% (approximately 5–10% higher at low Pr (= 5) and 5–10% lower at high Pr (= 100) for all Re between 10^4 and 10^6). These differences are similar to those between the correlation and the best available experimental data [11]. The entrance length of 3–4 the diameter for the case of water is also comparable to those obtained experimentally by Hartnett [12] and theoretically by Sparrow et al. [13]. Careful grid size independence studies were also conducted to verify the validity of the solutions. These showed that a Δr of 10^{-4} was acceptable for $Re \leqslant 10^5$, whereas a Δr of 10^{-5} was used for $Re = 10^6$. The solutions were independent of Δx less than 10^{-2} for all Re and Pr combinations. Two versions of the program were developed during the testing phase, one assuming that the turbulent Prandtl number is 1 (i.e. the Reynolds analogy holds or $\epsilon_m/\epsilon_H = 1$), and other using a semi-empirical equation for the turbulent Prandtl number [14]. As expected, the numerical results with both models are similar since

the Prandtl numbers under consideration significantly greater than 1. Thus, all numerical runs were done assuming a turbulent Prandtl number of 1.

4. Results and discussions

Experimental data for turbulent heat transfer to PCM suspensions have been reported by Choi [15,16]. In order to verify the model, numerical solutions were obtained for non-dimensional parameters corresponding to these experiments. The concentration, density, thermal conductivity and specific heat capacity for *n*-hexadecane were obtained directly from [15]. Properties of water were at 15°C which was approximately the mean temperatures during the experiments. The latent heat, melting point, inlet temperature of the fluid and the flow rate were calculated from the experimental data in [15]. The viscosity was calculated using an available correlation for suspensions [17] using properties of water at 15°C which was approximately the mean temperature during the experiments. This value was also verified approximately by using friction factor data in [15]. Alternative correlation for emulsions were also used [18] but the differences between the predictions were quite small (<10%).

One particular parameter, the melt temperature range posed some problems at the initial stages of verification. However, since the phase change material, *n*-hexadecane, was not a mixture but a single component substance (possibly with some impurities, see later section), physical considerations suggest that the melt temperature range will be of the order of 1–2°C or lower. Numerical runs with the corresponding non-dimensional melt temperature range showed that the results were insensitive to the actual value and the final results correspond to an $Mr = 0.0035$.

Fig. 1(a) shows the wall temperature rise along the length of the tube as predicted by the model together with the experimental data from [15]. The difference between the two results are within 10–20% over the entire length of the tube. These are noticeably greater than those associated with results for a pure fluid where the model predictions are typically within 10% of experimental results. However, a careful analysis points to probable reasons for these higher discrepancies. First, consider the dashed lines which have been drawn parallel to the numerical predictions for the two cases. Note that these follow the measured temperatures quite accurately (less than 1°C difference) except at the later stages of the 12.3 kW experiment. In this high power experiment, the difference between the dashed line and the experimental data can be seen to increase gradually with increasing temperatures. Based on these observations, the overall differences can be attributed to two factors: (a) a temperature difference that is uniform

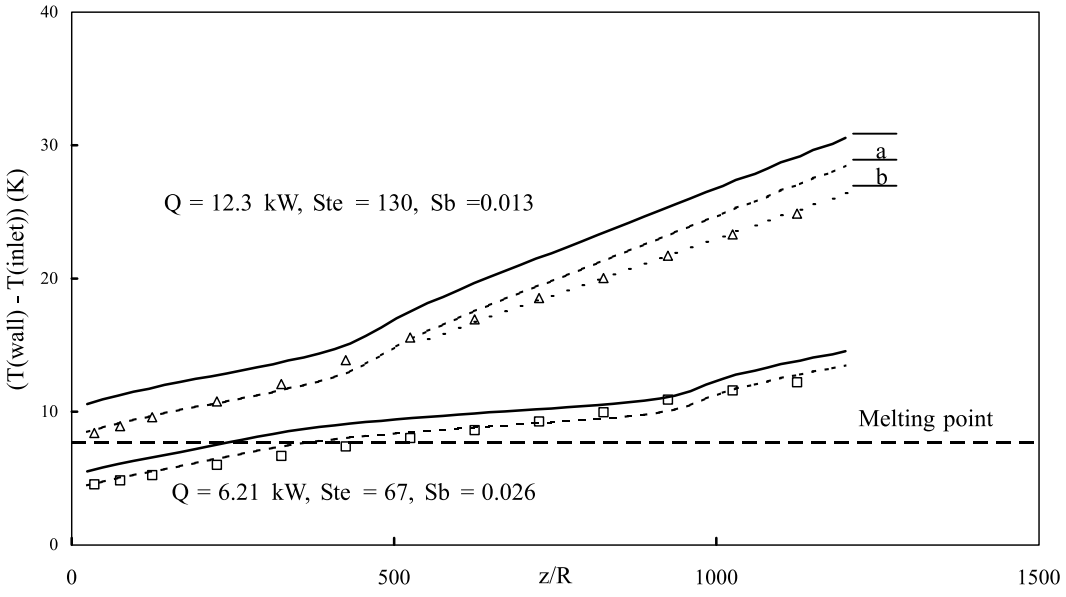

Fig. 1. Comparison of numerical predictions with experimental data of Choi [15]. Water: $c_p = 4.19 \times 10^3$ J/kg K, $k = 0.593$ W/m K, $\rho = 999$ kg/m^3, $\mu = 1.16 \times 10^{-3}$ N s/m^2. *n*-hexadecane: $c_p = 1.92 \times 10^3$ J/kg K, $k = 0.144$ W/m K, $\rho = 773$ kg/m^3, $h_{fs} = 2.19 \times 10^5$ J/kg, Melting point = 16.5°C. Suspension: $c = 0.1$, $c_m = 0.079$, $c_p = 4.01 \times 10^3$ J/kg K, $k = 0.535$ W/m K, $\rho = 976$ kg/m^3, $\mu = 1.55 \times 10^{-3}$ N s/m^2. Experimental parameters: $d = 0.01$ m, $u_m = 1.6$ m/s, $T_i = 8.8$°C, heated length = 6.37 m. Non-dimensional parameters: $Re = 10,200$, $Pr = 11.6$, $c_{p,ND} = 0.038$, $Mr = 0.0035$ (assumed same in both cases).

along the length of the tube; (b) a gradually increasing difference that occurs primarily at higher temperatures. These are considered separately below:

(a) The constant temperature difference is present even in the early sections of the tube. *Since the fluid/wall temperatures are below the reported melting point of n-hexadecane in this region* (*a point that is particularly noticeable for the* 6.21 kW *test*), *this discrepancy between the experimental results and the numerical predictions cannot be due to any limitations in the effective specific heat capacity model*. Instead, thermodynamic considerations suggest that this is probably due to phase change effects at lower temperatures caused by impurities in the commercial grade material used in the experiments. This explanation is also supported by the fact that the melting point of the *n*-hexadecane (16.5°C) in the suspension was lower than that of a laboratory grade sample (18.1°C). Quantitative verification of any form is unfortunately not possible since DSC or other test data has not been reported for this material (though the presence of unknown impurities is confirmed in [15]).

(b) The source of the gradually increasing "error" in the high power test is much easier to identify. In this experiment, the temperatures ranged from about 9–33°C due to the high heat flux. Although most properties of water do not change significantly over this temperature range, the viscosity does decrease by about 60%. As a result, the Reynolds number associated with the flow changes significantly along the length of the tube. Under these circumstances, Choi and Cho [19] have shown that the Nusselt numbers along the length of the tube can differ from the fully developed values by as much as 20%. The corresponding wall temperatures will also be affected similarly, and the differences between the predictions from a constant property model and experimental data will be larger than expected at high temperatures.In order to verify this hypothesis, it is useful to consider a correlation for the local Nusselt number, Nu_z that accounts for this axial variation in viscosity [19]:

$$Nu_z = 0.00425 Re_z^{0.979} Pr_z^{0.4} (\mu_m/\mu_w)^{0.11}.$$

In this equation, Re_z and Pr_z are the *local* Reynolds and Prandtl numbers based on the bulk properties at a given axial position z/R on the tube. Since the wall temperature rise is inversely proportional to the local Nusselt number, it is possible to estimate a corrected wall temperature by using the following equation:

$$(T_w - T_m)_{z,COR} = \left[\frac{\mu_{m,z}}{\mu_{15°C}}\right]^{0.469} \left[\frac{\mu_{w,z}}{\mu_{15°C}}\right]^{0.11} (T_w - T_m)_{z,CP},$$

where the subscripts COR and CP refer to the corrected temperatures and the temperatures obtained using the constant property model, respectively. Wall temperatures have been calculated using the above equation and are also shown superimposed on the dashed line in Fig. 1. Note that the modified temperature distribution now clearly follows the experimental data very well.

The above results and analysis provide a reasonably good verification of the effective specific heat model used in this study. The fact that a relatively simple model can provide quantitative results that predict the pattern of the experimental data is particularly notable since the model can be used for future design if it is further verified through systematic experimental studies. In order to provide such data to support future experiments (and initial systems design), a parametric study has been done to evaluate the performance of PCM suspensions under various operating conditions.

The primary parameter influencing the heat transfer was found to be the Stefan number with 50% or greater reductions possible in the wall temperature rise for Stefan numbers as high as 50–100 for z/R of the order of 100–250 (Fig. 2). For lower Stefan numbers, of the order of 5–10, wall temperatures may be reduced by 80% or more for lengths of the order of 1500–2000 diameters or more. Fig. 2 also shows that the phase change effects are concentrated over tube lengths that are approximately inversely proportional to the Stefan number (z/R of 1400, 350 and 175 for *Ste* of 10, 50 and 100, respectively).

The melt temperature range, *Mr*, determines the heated length over which the phase change effects are apparent. When *Mr* values are small, i.e. for suspensions with phase change materials melting over a small temperature range and/or for systems with high heat fluxes, the phase change effects are limited to a smaller region of the tube. However, the localized temperature reductions are higher for these cases as seen in Fig. 3. For higher melt temperature ranges/lower heat fluxes, the *relative* wall temperature reductions are somewhat lower (for the same Stefan number) but are felt over a greater section of the heated length. For most practical cases with high heat fluxes however, *Mr* will be very small and the Stefan number will be the only parameter determining the tube length over which the phase change effects are important.

The degree of subcooling directly influences the region of the tube that is affected by the phase change process. As its value increases, the melting effects are seen further downstream (Fig. 4). The relative temperature reductions therefore tend to be higher for lower subcooling. An important point to note is that approximately 50% of the phase change effects are complete by z/R equal to $RePrSb/4$ (i.e. at $z/r = 125$, 250 and 1250 for $Sb = 0.005$, 0.01 and 0.05, respec-

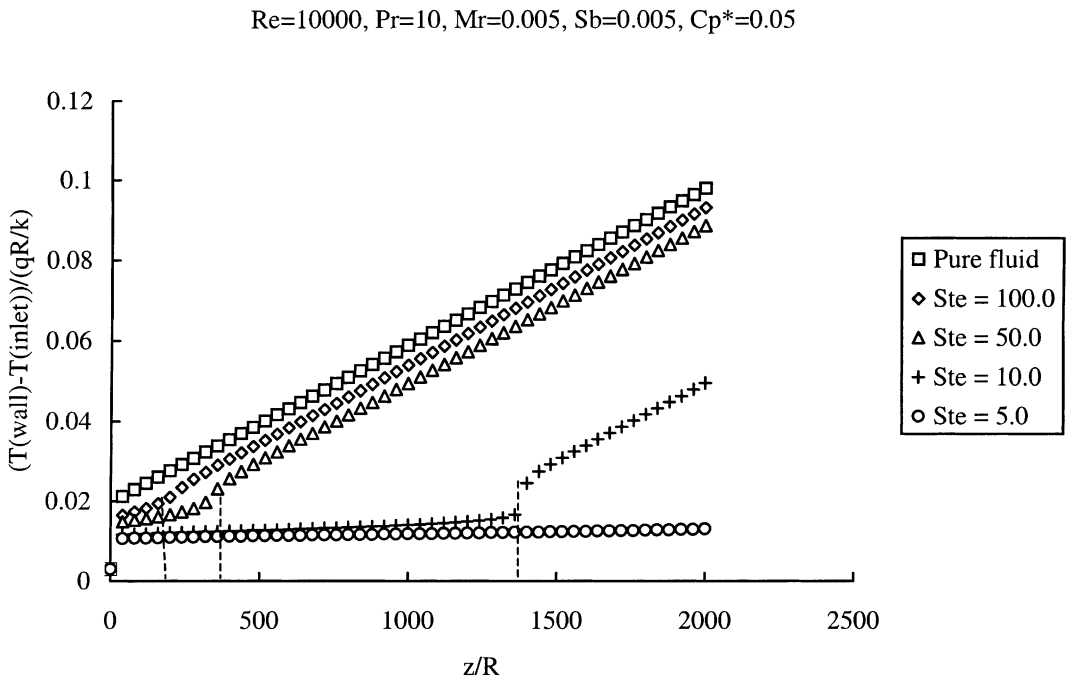

Fig. 2. Wall temperature variations along tube for various Stefan numbers: $Re = 10{,}000$, $Pr = 10$, $Mr = 0.005$, $c_{p,ND} = 0.05$.

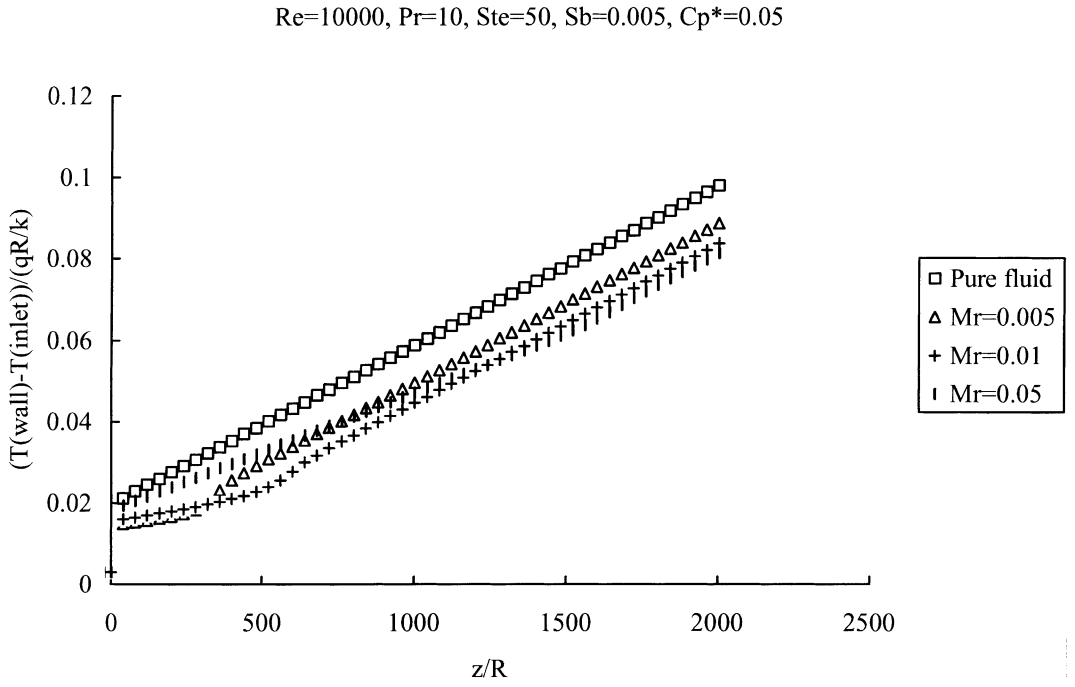

Fig. 3. Wall temperature variations along tube for various melt temperature ranges: $Re = 10{,}000$, $Pr = 10$, $Ste = 50$, $Sb = 0.005$, $c_{p,ND} = 0.05$.

tively). This corresponds to the location where the phase change material would begin melting if the fluid were perfectly mixed. It is also the location where the Nusselt number achieves a maximum value based on the three-equation bulk mean temperatures suggested by Choi [15,16].

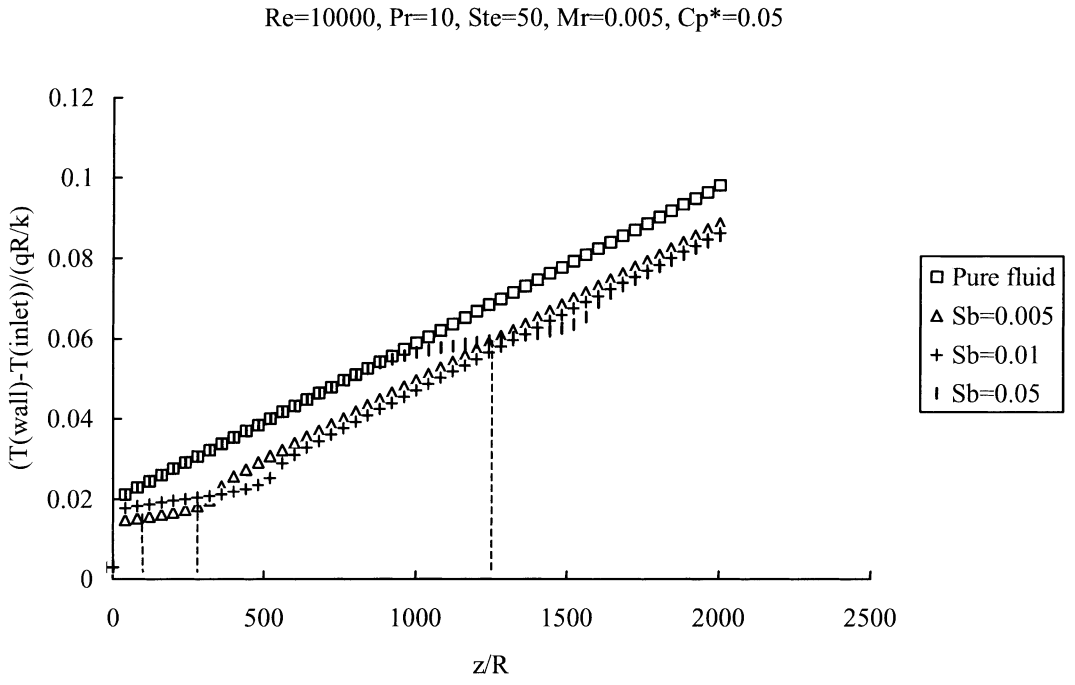

Fig. 4. Wall temperature variations along tube for various degrees of subcooling: $Re = 10{,}000$, $Pr = 10$, $Ste = 50$, $Mr = 0.005$, $c_{p,ND} = 0.05$.

Finally, the numerical results also showed that the specific heat ratio does not have a significant impact on the heat transfer process. A careful consideration of α_{ND} shows that this is inevitable since $c_{p,ND}$ is typically much smaller than 1 (as is the product $Ste \cdot Mr(1 - c_{p,ND})$ in many cases). Thus, the normalized wall temperature distributions and Nusselt numbers will be functions of only three parameters, *Ste*, *Sb* and *Mr*. For high heat fluxes and/or suspensions with relatively pure phase change materials resulting in very low values of *Mr*, only the first two parameters (and if necessary, the Reynolds and Prandtl numbers) will be of importance. Although it is feasible to develop correlations for the normalized wall temperatures and Nusselt numbers using the numerical model, such correlations have not been obtained since the available experimental data is too limited to permit proper calibration. The initial quantitative results discussed in this paper will hopefully provide a basis for careful parametric experimental studies in the future.

5. Conclusions

This study has shown that an effective specific heat capacity model can be effectively used to model turbulent heat transfer with phase change material suspensions. The Stefan number found to be the primary parameter influencing the heat transfer process. Considerable reductions in wall temperatures are seen over large heated lengths for low to moderate Stefan numbers. The melt temperature range and degree of subcooling are two other important parameters with the degree of subcooling determining the location of the phase change effects. Non-dimensional operating parameters/tube locations where phase change effects are important can be estimated from the numerical results. Further experimental research together with DSC tests to properly characterize the phase change materials are recommended so that the numerical models can be accurately calibrated.

Acknowledgements

This material is based upon work supported by U.S. Army Tank-Automotive and Armaments Command under Contract No. DAAE07-98-C-L021 and DAAE07-96-C-X021. Any opinions, findings and conclusions or recommendations expressed in this material are those of the authors and do not necessarily reflect the view of U.S. Army TACOM. Mr. H. Pangilinan at U.S. Army TACOM was particularly helpful in identifying areas of research and possible applications of this work.

References

[1] J.C. Mulligan, D.P. Colvin, Y.G. Bryant, Microencapsulated phase-change material suspensions for heat transfer

in spacecraft thermal systems, J. Spacecraft Rockets 33 (1996) 278–284.
[2] Y. Zhang, A. Faghri, Analysis of forced convection heat transfer in microencapsulated phase change material suspensions, J. Thermophysics Heat Transfer 9 (1995) 727–732.
[3] E.L. Alisetti, S.K. Roy, Forced convection heat transfer to phase change material slurries in circular ducts, J. Thermophysics Heat Transfer 14 (2000) 115–118.
[4] P. Charunyakorn, S. Sengupta, S.K. Roy, Forced convection heat transfer in microencapsulated phase change material slurries: flow in circular ducts, Int. J. Heat Mass Transfer 34 (1991) 819–833.
[5] C. Orr Jr., J.M. Dallavalle, Heat-transfer properties of liquid–solid suspensions, Chem. Eng. Progress Sympos. 50 (9) (1954) 29–45.
[6] G.C.J. Bart, P.C. van der Laag, Modeling of arbitrary-shaped specific and latent heat curves in phase-change storage simulation routines, Trans. ASME, J. Solar Energy Eng. 112 (1990) 29–33.
[7] B. Wunderlich, Thermal Analysis, Academic Press, San Diego, CA, 1990 (Chapter 4).
[8] M.S. Bhatti, R.K. Shah, Turbulent and transition flow convective heat transfer, in: S. Kakac, R.K. Shah, W. Aung (Eds.), Handbook of Single-Phase Convective Heat Transfer, Wiley, New York, 1987 (Chapter 4).
[9] T. von Karman, The analogy between fluid friction and heat transfer, Trans. ASME 61 (1939) 705–710.
[10] E.R. van Driest, On turbulent flow near a wall, J. Aeronautical Sci. 23, (1956) 1007–1011, 1036.
[11] B.S. Petukhov, Heat transfer and friction in turbulent pipe flow with variable physical properties, in: J.P. Hartnett, T.F. Irvine Jr. (Eds.), Advances in Heat Transfer, vol. 6, Academic Press, New York, 1970, pp. 503–564.
[12] J.P. Hartnett, Experimental determination of the thermal-entrance length for flow of water and of oil in circular pipes, Trans. ASME 77 (1955) 1211–1220.
[13] E.M. Sparrow, T.M. Hallman, R. Siegel, Turbulent heat transfer in the thermal entrance region of a pipe with uniform heat flux, Appl. Sci. Res. Series A 7 (1957) 37–52.
[14] W.M. Kays, M.E. Crawford, Convective Heat and Mass Transfer, 2nd ed., McGraw-Hill, New York, 1980 (Chapter 13).
[15] E. Choi, Forced convection heat transfer with water and phase-change-material slurries: turbulent flow in a circular tube, Ph.D. Thesis, Drexel University, PA, 1993.
[16] E. Choi, Y.I. Cho, H.G. Lorsch, Forced convection heat transfer with phase-change-material slurries: turbulent flow in a circular tube, Int. J. Heat Mass Transfer 17 (1994) 207–215.
[17] V. Vand, Theory of viscosity of concentrated suspensions, Nature 155 (1945) 364–365.
[18] P. Vergne, M. Kamel, M. Querry, Behavior of cold-rolling oil-in-water emulsions: a rheological approach, Trans. ASME, J. Tribology 119 (1997) 250–258.
[19] E. Choi, Y.I. Cho, Local friction and heat transfer behavior of water in a turbulent pipe flow with a large heat flux at the wall, Trans. ASME, J. Heat Transfer 117 (1995) 283–288.